IL22 furthers malignant transformation of rat mesenchymal stem cells, possibly in association with IL22RA1/STAT3 signaling

XIANGRONG CUI[1-3], XUAN JING[4], QIN YI[1-3], ZHONGPING XIANG[1-3], JIE TIAN[5], BIN TAN[1-3] and JING ZHU[1-3]

[1]Ministry of Education Key Laboratory of Child Development and Disorders, Pediatric Research Institute;
[2]China International Science and Technology Cooperation Base of Child Development and Critical Disorders;
[3]Chongqing Key Laboratory of Pediatrics, Children's Hospital of Chongqing Medical University, Chongqing 400014;
[4]Clinical Laboratory, Shanxi Province People's Hospital, Taiyuan, Shanxi 030001;
[5]Cardiovascular Department (Internal Medicine), Children's Hospital of Chongqing Medical University, Chongqing 400014, P.R. China

Received September 4, 2018; Accepted February 5, 2019

DOI: 10.3892/or.2019.7007

Abstract. Mesenchymal stem cells (MSCs) hold great promise as potential therapies for tumors through the delivery of various anticancer agents. However, exogenous tissue-derived MSCs, such as those of bone marrow, have exhibited a tendency for malignant transformation in the tumor microenvironment. This issue remains controversial and is poorly understood. In the present study, the role of interleukin 22 (IL22)/IL22 receptor subunit α 1 (IL22RA1) and signal transducer and activator of transcription 3 (STAT3) signaling in the malignant transformation of MSCs was investigated. Following isolation of rat MSCs and their indirect co-culture with C6 glioma cells, the transformed MSCs exhibited tumor cell characteristics. The Cancer Genome Atlas-Glioblastoma Multiforme analysis revealed that primary and recurrent glioblastomas have increased IL22RA1 expression, compared with normal tissues, whereas the expression of IL22 was low in glioblastoma and normal tissues. mRNA and protein expression levels of IL22RA1 were significantly increased in the MSCs co-cultured with C6 glioma cells. Furthermore, MSCs incubated with IL22 exhibited increased proliferation, migration and invasion. STAT3 demonstrated activation and nuclear translocation in the presence of IL22. Additionally, STAT3 small interfering RNA significantly inhibited the migration and invasion ability of MSCs, and the expression of the STAT3 downstream targets cyclin D1 and B-cell lymphoma-extra large under IL22 stimulation, indicating that IL22 also promoted MSC migration and invasion through STAT3 signaling. These data indicated that IL22 serves a critical role in the malignant transformation of rat MSCs, which is associated with an enhancement of the IL22RA1/STAT3 signaling pathway in the tumor microenvironment.

Correspondence to: Dr Jing Zhu, Ministry of Education Key Laboratory of Child Development and Disorders, Children's Hospital of Chongqing Medical University, 136 Zhongshan 2nd Road, Yuzhong, Chongqing 400014, P.R. China
E-mail: jingzhu@cqmu.edu.cn

Key words: interleukin 22, interleukin 22 receptor subunit α 1, signal transducer an activator of transcription 3, mesenchymal stem cells, tumor microenvironment

Introduction

Malignant glioma is the most frequent and lethal type of primary tumor of the central nervous system (1-3). Despite improvements in therapeutic technologies, the current treatment strategies remain poorly effective. Increasing evidence indicated that mesenchymal stem cells (MSCs) preferentially migrate to and engraft into tumor sites and interact with tumor microenvironments, which, in addition to their availability, immunological compatibility and relative ease of *in vitro* manipulation without the need for immortalization, indicates these cells as the most attractive candidates for tumor therapy (4-6).

Although MSCs have high potential for application in tumor therapy, a number of adverse effects have been demonstrated in the context of their direct and indirect involvement in the tumor microenvironment (6-9). In the tumor niche, MSCs interact with tumor cells and may promote angiogenesis, tumor growth, migration, invasion and metastasis (6-9). MSCs can also undergo malignant transformation following long-term *in vitro* culture (10). Furthermore, in tumor microenvironment, MSCs can undergo malignant transformation, through increased migration and invasion abilities, increased proliferating capacity, and form tumors in immunocompromised mice (7-9).

In our previous studies, it was demonstrated that MSCs can undergo malignant transformation through migration and invasion abilities, *in vivo* tumorigenesis and growth, with

S100B/advanced glycosylation end-product specific receptor serving a role by activating the interleukin 6 (IL6)/signal transducer and activator of transcription 3 (STAT3) signaling pathway (7-9). However, in addition to tumor cells, numerous tumor immune cells, including monocytes, macrophages, mast cells, microglia and neutrophils, serve indispensable roles in the initiation and progression of glioblastoma in the tumor microenvironment (10-12).

In the central nervous system, the presence of human T helper (Th)17 lymphocytes and their deleterious role were described in multiple sclerosis lesions (13). Liu *et al* (13) reported the expression of IL17 and IL22 receptors on blood-brain barrier endothelial cells during multiple sclerosis lesions and in experimental autoimmune encephalomyelitis, a mouse model of multiple sclerosis. IL22, a member of the IL10 cytokine family, is produced by a number of subsets of lymphocytes, including γδ T cells, Th22 cells, Th17 cells, natural killer T cells, innate lymphoid cells and $CD8^+$ lymphocytes (14). IL22 appears to act exclusively on non-hematopoietic cells, expressing a heterodimer transmembrane complex composed of IL22RA1 and IL10RB subunits (15). IL22RA1 is almost entirely expressed on cells of non-hematopoietic origin (16). The primary signaling pathway downstream of IL22RA1 is the STAT3 cascade, which mediates the majority of IL22-induced effects, including promotion of tumor growth and metastasis, as well as inhibition of apoptosis (14). Furthermore, Seki *et al* (17) demonstrated that IL22 attenuates double-stranded RNA-induced upregulation of programmed death-ligand 1 in airway epithelial cells via a STAT3-dependent mechanism. Thus, it has been concluded that in the glioma microenvironment, the occurrence and development of glioma is not only associated with glioma cells, but also involves IL22 secreted by Th17 lymphocytes and other immune cells. It was hypothesized that IL22 produced by immune cells would activate the STAT3 cascade through interaction with IL22RA1, to promote the malignant transformation of MSCs. Therefore, the characteristics of transformed malignant MSCs and the mechanism underlying their transformation were evaluated, thereby highlighting the safety issues to be addressed prior to the clinical application of MSCs.

Materials and methods

MSC isolation, culture, and transfection. Male Sprague Dawley rats (n=40; 4-week-old; 40±10 g each; from the Experimental Animal Center of Chongqing Medical University, Chongqing, China) were kept at 23±3˚C and 55±5% humidity, with normal diet and regular drinking water. A 12/12 h light/dark cycle used for all rats. The rats were euthanized through intraperitoneal injection of a mixture solution of ketamine (87.5 mg/kg) and xylazine (12.5 mg/kg), and the bone marrow aspirates were separated and cultivated by the plastic adherence method (18). All experiments using rats were approved by the Medical Research Ethics Committee of Chongqing Medical University for the Ethics of Animal Experiments of Chongqing Medical University. MSCs were cultured in Dulbecco's modified Eagle's medium (DMEM)/F12 containing 10% fetal bovine serum (FBS; both from Gibco; Thermo Fisher Scientific, Inc., Waltham, MA, USA) and incubated at 37˚C in an atmosphere containing 5% CO_2 and 95% humidity. At 70-80% confluence, the cells were subcultured for four passages and harvested for phenotypic characterization and differentiation as described previously (13). MSC phenotypes were analyzed with a flow cytometer (BD FACSCanto; BD Biosciences; Becton, Dickinson and Company, Franklin Lakes, NJ, USA), according to the subsequent protocol. Cells were trypsinized and incubated with fluorescein isothiocyanate (FITC)-conjugated monoclonal anti-rat cluster of differentiation 71 (CD71; 1:100; cat. no. 554890; BD Biosciences; Becton, Dickinson and Company), CD90 (1:100; cat. no. 554894; BD Biosciences; Becton, Dickinson and Company), CD45 (1:100; cat. no. 561867; BD Biosciences; Becton, Dickinson and Company) and phycoerythrin-conjugated mouse anti-rat CD34 (1:200; cat. no. AM20322RP-N; OriGene Technologies, Inc., Rockville, MD, USA).

Small-interfering RNA (siRNA) targeting rat STAT3 (si-STAT3) and the corresponding negative control (si-NC) were designed and synthesized by Shanghai GeneBio Co., Ltd. (Shanghai, China). For the transfection procedure, MSCs were grown to 80-90% confluence and transfected with 25 nM si-STAT3 and 25 nM negative control siRNA using Lipofectamine® 2000 (Invitrogen; Thermo Fisher Scientific, Inc.), according to the manufacturer's protocols. The target mRNA sequence for si-STAT3 was (5'-GGCAUAUGCAGC CAGCAA-3') and si-NC was (5'-UUUGCUGGCUGCAUA UGCC-3'). After incubation for 48 h, cells were washed with PBS, harvested and subjected to proliferation, western blot analysis, and invasion and migration assays.

Indirect co-culture of MSCs with rat glioma C6 cells. Rat C6 glioma cells were obtained from Children's Hospital Affiliated to Chongqing Medical University. MSCs were indirectly co-cultured with glioma cells using Transwell chambers (EMD Millipore, Billerica, MA, USA). A total of $3x10^5$ C6 cells (in 200 μl DMEM/F12 supplemented with 10% FBS) were seeded into the upper chamber of the Transwell plate (0.4 mm). An equal number of MSCs (in 200 μl DMEM/F12 supplemented with 10% FBS) was seeded in the lower part of the chamber. After 7 days of indirect co-culture with C6 cells, the MSCs were collected for analysis. MSCs cultured alone served as the control. The cells were imaged under a confocal microscope (magnification, x100; Eclipse Ti2; Nikon Corporation, Tokyo, Japan).

Cell Counting Kit-8 (CCK-8) detection of viability. Cell viability was assayed with CCK-8 (Chongqing ATGene Pharmaceutical Technology Co., Ltd., Chongqing, China), following the manufacturer's protocols. MSCs and C6 glioma cells were seeded in 96-well plates ($1x10^4$ cells/well) and cultured in 100 μl serum-free DMEM/F12 medium for 1, 2, 3, 4, 5, 6 and 7 days, or a 24 and 48 h incubation of MSCs with exogenous IL22 (Abcam, Cambridge, MA, USA) at 37˚C. Subsequently, the cells were incubated with 10% CCK-8 solution for 2 h at 37˚C and the absorbance value was measured at 450 nm using a microplate reader (BioTek Instruments, Inc., Winooski, VT, USA). All measurements were conducted with eight replicates and each experiment was repeated at least three times.

Cell migration and invasion. For invasion and migration assays, $1x10^5$ cells in serum-free DMEM/F12 medium were

placed into the upper chamber of a Transwell plate (24-well; 8-mm pore size) coated with or without Matrigel, respectively. DMEM/F12 medium containing 10% FBS was added to the lower chamber. After incubation for 24 h, the cells remaining on the upper membrane were removed with cotton wool. The cells that had migrated or invaded through the membrane were fixed with 4% paraformaldehyde for 30 min at 37˚C and stained with 0.1% crystal violet for 4 h at 37˚C (Beyotime Institute of Biotechnology, Shanghai, China), imaged and counted using an inverted microscope (magnification, x100; Eclipse Ti2; Nikon Corporation).

Cell cycle and flow cytometry. Cell cycle distribution was analyzed using a flow cytometer (BD FACSCanto). Cells were pooled and placed in tubes at a density of $1.6x10^5$ cells/tube. The cells were fixed in 70% ethanol for 24 h at 4˚C and washed three times with PBS. Finally, the cell pellets were tested by Cell Cycle kit (Thermo Fisher Scientific, Inc.), incubated with RNase (1 mg/ml; Thermo Fisher Scientific, Inc.) and 400 μl propidium iodide solution (100 μl/ml; Thermo Fisher Scientific, Inc.) for 30 min at 37˚C in the dark and analyzed by flow cytometry using ModFit LT software (version 3.2; Verity Software House, Inc., Topsham, ME, USA). Each experiment was repeated at least three times.

ELISA. Secreted IL22 was measured in the supernatant of the C6 glioma cell and MSC culture medium using an ELISA. The ELISA (cat. no. E-EL-R2440c; Elabscience Biotechnology Co., Ltd., Wuhan, China) was performed according to the manufacturer's protocols, and the results were analyzed with SoftMax® Pro-5 (Molecular Devices, LLC, Sunnyvale, CA, USA). Concentrations below the detection limit (5 pg/ml) were considered undetectable.

Reverse transcription-quantitative polymerase chain reaction (RT-qPCR) analysis. Total RNA was extracted using an RNA extraction kit (BioTeke Corporation, Beijing, China), and cDNA synthesis was conducted with a PrimeScript™ RT Master Mix kit, according to the manufacturer's protocols (Takara Biotechnology Co., Ltd., Dalian, China). RT-qpcr was performed in three replicates using a SYBR® Premix Ex Taq Kit (Takara Bio, Inc., Tokyo, Japan), according to the manufacturer's protocol using gene-specific primers, and products were measured on a CFX96 Real-time PCR system (Bio-Rad Laboratories, Inc., Hercules, CA, USA). The primers used were as follows: IL22RA1, forward, 5'-CTGTGGAGACCCGAAAC-3', and reverse, 5'-GCACCCGAGAAGGAGT-3'. GAPDH (forward, 5'-ACCACAGTCCATGCCATCAC-3'; and reverse, 5'-TCCACCACCCTGTTGCTGTA-3') was used as the endogenous housekeeping gene for normalization of mRNA levels. The results are expressed as the mean of $2^{-\Delta\Delta Cq}$ ± standard deviation (19). The PCR amplification was performed as follows: 95˚C for 5 min; 35 cycles of 95˚C for 1 min, 60˚C for 1 min and 72˚C for 1 min; and then 72˚C for 7 min.

Immunofluorescence staining. Cells were seeded in 24-well plates ($4x10^4$ cells/well) DMEM/F12 medium containing 10% FBS for 24 h at 37˚C. Subsequently, they were then fixed with 4% paraformaldehyde for 1 h at 37˚C, permeabilized with 0.5% Triton X-100, and blocked for 1 h at 37˚C with 5% bovine serum albumin (Gibco; Thermo Fisher Scientific, Inc.). Following this, the cells were incubated overnight at 4˚C with the primary antibodies. Primary antibodies against STAT3 (cat. no. 12640; 1:200), phospho(p)-STAT3 (cat. no. 9134; 1:200), B-cell lymphoma-extra large (Bcl-xL, cat. no. 2764; 1:200) and cyclin D1 (cat. no. 2922; 1:200) were obtained from Cell Signaling Technology, Inc. (Danvers, MA, USA). Following a PBS wash, the cells were incubated with FITC (cat. no. S0008) or Cy3 (cat. no. S0011) conjugated goat anti-rabbit IgG secondary antibodies for an additional 2 h at 37˚C before being washed with PBS again at 37˚C three times in the dark. Secondary antibodies were also obtained from Affinity (1:200; Affinity Biosciences, Cambridge, UK). Subsequently, 20 μl 4',6-diamidino-2-phenylindole (DAPI; Beyotime Institute of Biotechnology) was added to stain the nuclei at 37˚C for 1 h. Images were obtained with a A1R Confocal microscopy system (magnification, x100; Nikon Corporation) and analyzed with Nikon NIS-element AR 4.0 software (Nikon Corporation).

Western blot analysis. Cell lysates (Whole Protein Extraction kit; Nanjing KeyGen Biotech Co., Ltd., Nanjing, China) were collected and a Bicinchoninic Acid protein assay (Nanjing KeyGen Biotech Co., Ltd.) was performed to determine protein concentrations. Proteins (40 μg) were separated on 8% SDS-PAGE and then transferred onto polyvinylidene fluoride membranes (EMD Millipore). Subsequently, the polyvinylidene fluoride membranes were blocked for 1 h in TBS containing 0.1% Tween-20 at room temperature with 5% fat-free milk. The following commercial antibodies were used to incubate membranes overnight at 4˚C: STAT3 (cat. no. 12640; 1:1,000; Cell Signaling Technology, Inc.), p-STAT3 (cat. no. 9134; 1:1,000; Cell Signaling Technology, Inc.), cyclin D1 (cat. no. 2922; 1:1,000; Cell Signaling Technology, Inc.), and Bcl-xL (cat. no. 2764; 1:1,000; Cell Signaling Technology, Inc.) and GAPDH (cat. no. T0004; 1:5,000; Affinity Biosciences). Subsequently, membranes were incubated with goat anti-rabbit IgG horseradish peroxidase-conjugated secondary antibodies (1:5,000; cat. no. SA00001-2; ProteinTech Group, Inc., Chicago, IL, USA) for 2 h at 37˚C. Blots were developed with the chemiluminescent detection method by enhanced chemiluminescence Prime Western Blotting Detection reagent (cat. no. KGP1127; Nanjing KeyGen Biotech Co., Ltd). The band intensity of western blotting was measured by densitometry using the Quantity One software v4.6.7 (Bio-Rad Laboratories). The protein levels were normalized to the protein level of GAPDH, which was used as a loading control.

Bioinformatic analysis of the expression of IL22 and IL22RA1 in glioblastoma. Heat maps of IL22 and IL22RA1 expression were identified using The Cancer Genome Atlas-Glioblastoma Multiforme (TCGA-GBM) data with the University of California, Santa Cruz (UCSC) Cancer Genomics Browser (http://xena.ucsc.edu/) (20-24).

Statistical analysis. SPSS 20.0 software (IBM Corp., Armonk, NY, USA) was used to analyze data with independent sample Student's t-test or one-way analysis of variance analysis of variance test with post hoc contrasts by Student-Newman-Keuls

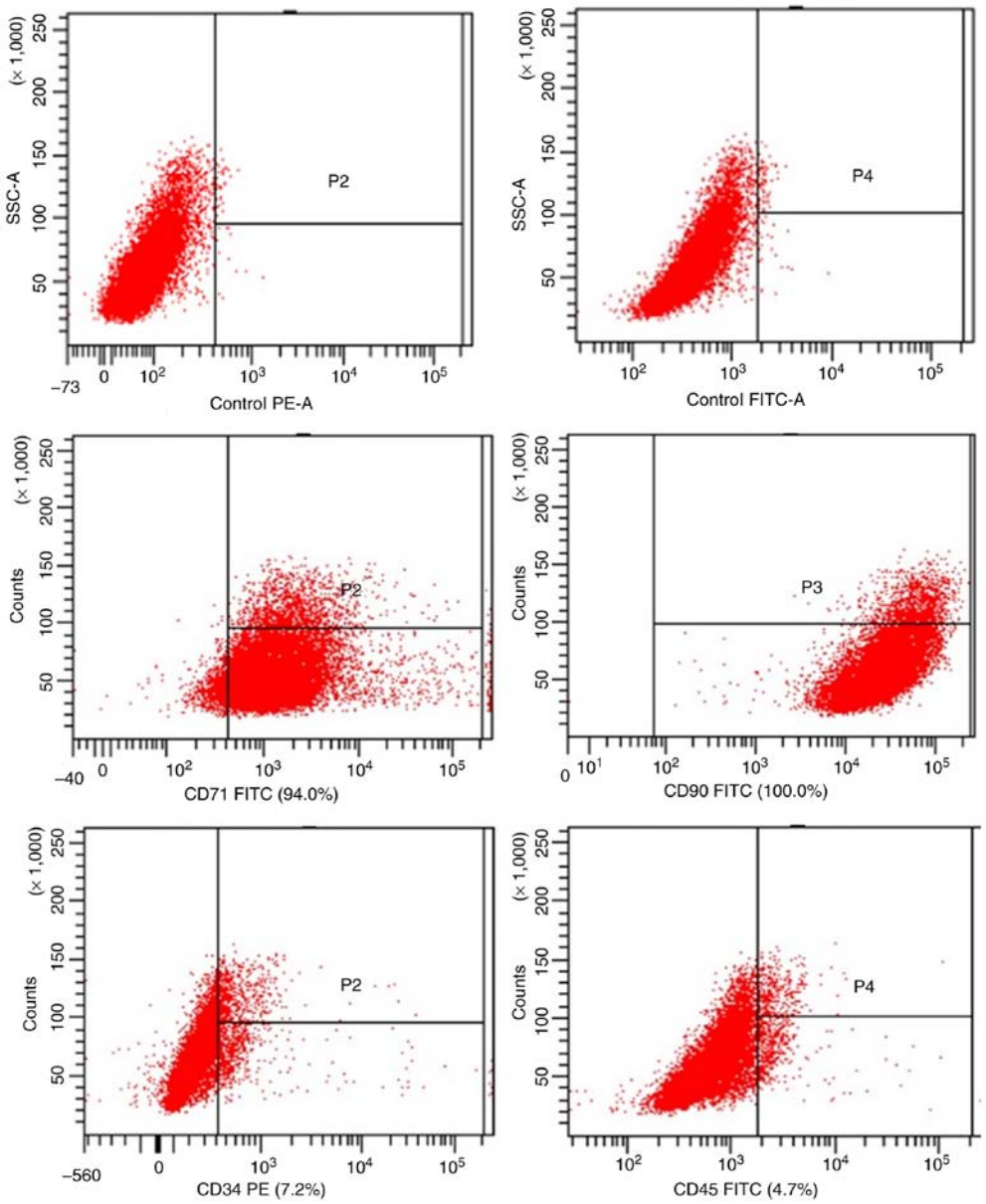

Figure 1. Phenotypic characterization of MSCs. Flow cytometric analyses of MSCs surface markers revealed that primary cells were positive for CD71 and CD90, while negative for CD34 and CD45. Control PE and Control FITC are the negative controls for PE and FITC staining, respectively. MSCs, mesenchymal stem cells; CD71, cluster of differentiation 71; FITC, fluorescein isothiocyanate; PE, phycoerythrin.

test. All values are reported as mean ± standard deviation of the mean. P<0.05 was considered to indicate a statistically significant difference.

Results

Identification of MSCs. To confirm that the cells used in the present study were MSCs, their phenotype was determined by measuring the specific cell surface markers CD71, CD90, CD34 and CD45. As depicted in Fig. 1, flow cytometric analyses revealed that the primary cultured MSCs were positive for CD7 and CD90 while negative for CD34 and CD45, indicating that they were MSCs.

Malignant transformation of MSCs in the simulated tumor microenvironment. Following long-term exposure to the tumor microenvironment, the MSCs exhibited numerous biological characteristics of C6 glioma cells, including altered cell morphology, and increased proliferation and invasion/migration ability. As depicted in Fig. 2A, the MSCs exhibited a typical long fusiform morphology, whirlpool and orderly arrangement. However, following long-term indirect co-culture with C6 glioma cells, the MSCs became thinner and longer with reduced cytoplasm around the nucleus, and an increased nuclear/cytoplasmic ratio. Therefore, they exhibited a similar shape to that of C6 glioma cells. Furthermore, MSCs co-cultured with C6 glioma cells exhibited an increased proliferation rate, compared with normal MSCs from day 4-6 (Fig. 2B). The flow cytometry results demonstrated that the percentage of MSCs in the G2/S phase was significantly increased following co-culture with C6 glioma cells, compared with the control group, indicating that cell proliferation was increased (P<0.05; Fig. 2C and D). Furthermore, MSCs co-cultured with C6 glioma cells exhibited a significantly

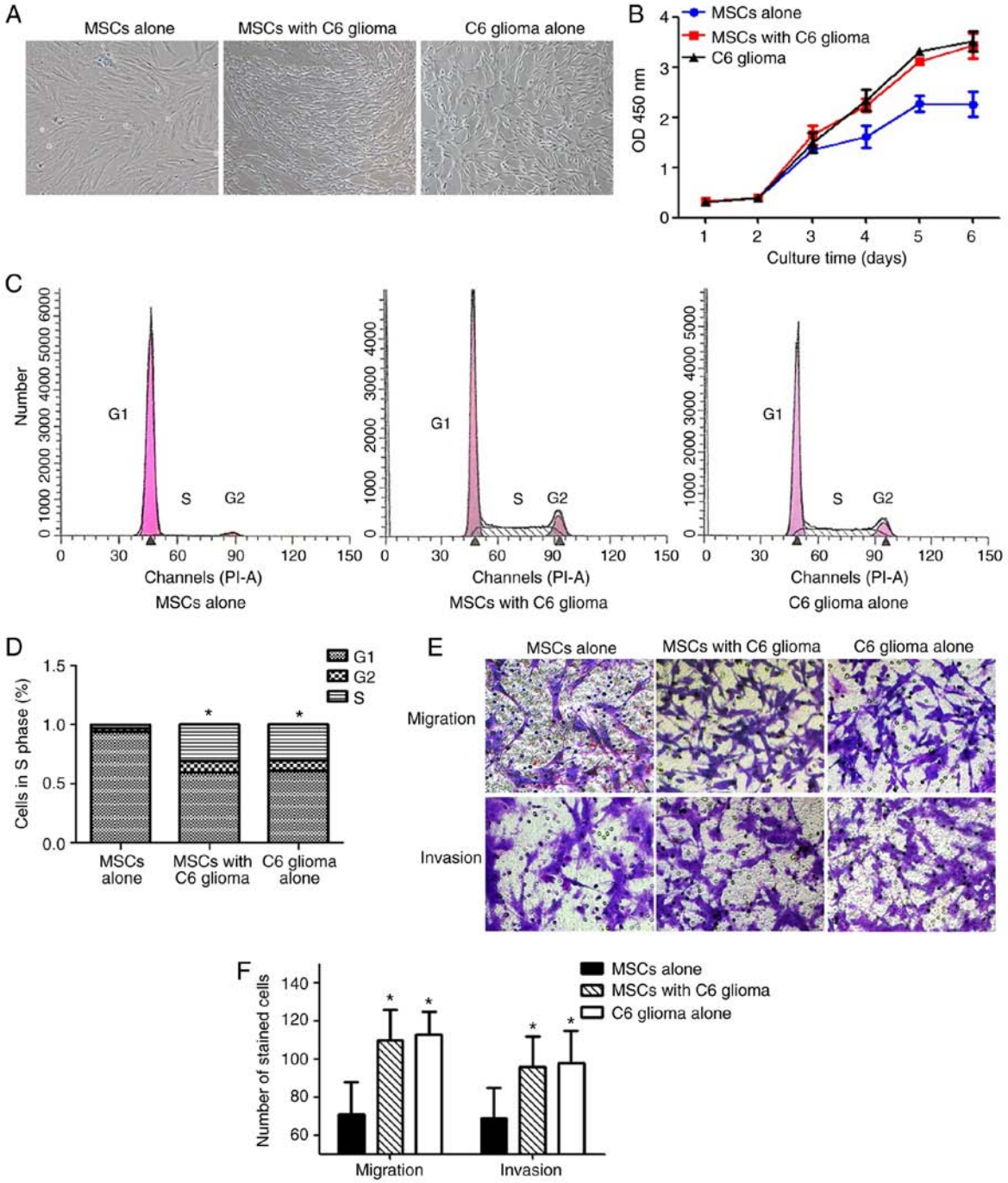

Figure 2. Alterations in the biological characteristics of MSCs following co-culture with C6 glioma cells. (A) Microscopic analysis revealed that MSCs exhibited tumor cell-like morphology at 1 month after indirect co-culture with C6 glioma cells. (B) A Cell Counting Kit-8 assay revealed that MSCs after indirect co-culture with C6 glioma cells had an increased cell proliferation rate, compared with MSCs alone, from day 4-6. (C) Flow cytometric analysis of cell cycle demonstrated the percentage of S phase cells was significantly increased in MSCs co-culturing with C6 glioma cells, compared with MSCs alone, which demonstrated that the proliferation capacity of MSCs is significantly enhanced following co-culturing with C6 glioma cells. (D) A quantitative presentation of the data depicted in (C). *P<0.05, compared with MSCs alone. (E) MSCs co-cultured with C6 glioma cells exhibited increased migration and invasion capacity, compared with normal MSCs. (F) Histogram of migration and invasion in three groups. MSCs, mesenchymal stem cells; OD, optical density; PI, propidium iodide.

increased migration and invasion capacity, compared with normal MSCs (both P<0.05; Fig. 2E and F).

Bioinformatics analysis of the expression of IL22 and IL22RA1 in glioblastoma. The expression profile of IL22 and IL22RA1 in TCGA-GBM was analyzed using the UCSC Cancer Genomics Browser (Fig. 3). The heatmap and the corresponding box plots depict that primary and recurrent glioblastomas have increased IL22RA1, expression compared with normal tissue (Fig. 3A and B), whereas the expression of IL22 was low in glioblastoma and normal tissues (Fig. 3A and C).

Expression of IL22RA1, not IL22, is increased in MSCs co-cultured with C6 glioma cells. Hepatocyte growth factor,

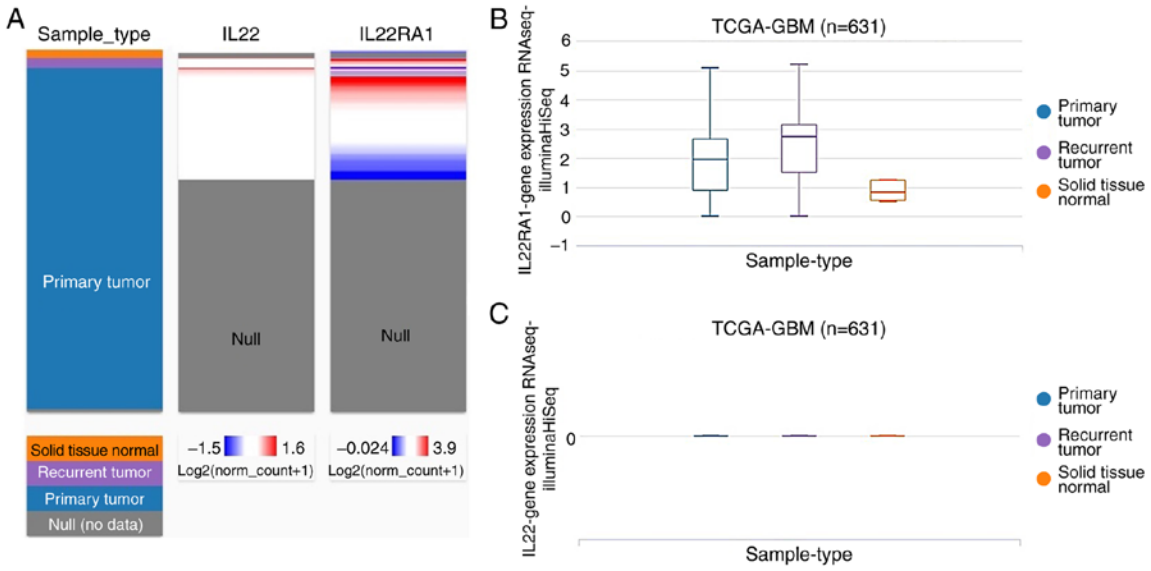

Figure 3. Bioinformatics analysis of the expression of IL22 and IL22RA1 in glioblastoma. (A) The heatmap of IL22 and IL22RA1 in glioblastoma and normal tissues. (B) Box plots of IL22RA1 expression in glioblastoma and normal tissues. (C) Box plots of IL22 expression in glioblastoma and normal tissues. TCGA-GBM, The Cancer Genome Atlas-Glioblastoma Multiforme; ILL22RA1, interleukin 22 receptor subunit α 1.

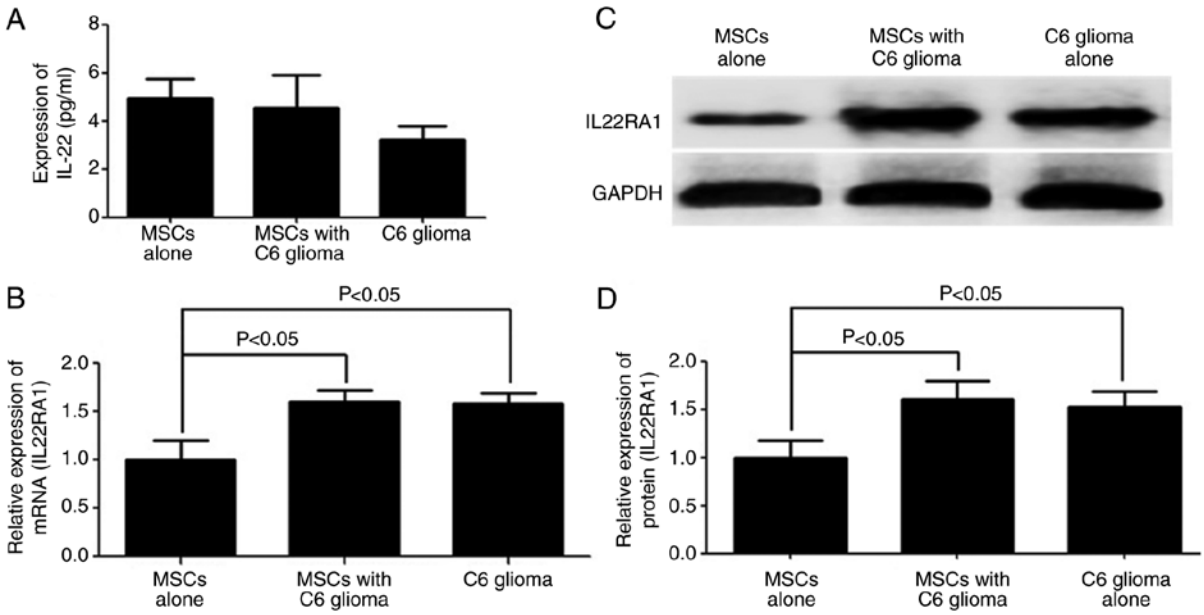

Figure 4. Expression of IL22 and IL22RA1 in MSCs co-cultured with tumor cells. (A) Analysis with ELISA indicated that IL22 was not detected (<5 pg/ml) in culture supernatant of C6 glioma cells and MSCs. (B) The mRNA expression of IL22RA1 was significantly increased in MSCs co-cultured with C6 glioma cells. (C) The protein expression of IL22RA1 was notably increased in MSCs co-cultured with C6 glioma cells. (D) Histogram of IL22RA1 protein expression in three groups. MSCs, mesenchymal stem cells; ILL22RA1, interleukin 22 receptor subunit α 1.

IL6 and S100B are highly secreted in MSCs co-cultured with C6 glioma cells, as demonstrated in previous studies (7-9). However, other cytokines may affect the MSCs phenotype. Thus, an ELISA was performed to detect the expression level of IL22, which is primarily produced by immune cells (17). IL22 was not detected (<5 pg/ml) in the culture supernatant of C6 glioma cells or MSCs, which is consistent with previous studies (25,26) (Fig. 4A). However, the mRNA and protein expression levels of IL22RA1 were significantly increased in the MSCs co-cultured with C6 glioma cells (Fig. 4B-D).

IL22 induces MSC proliferation, migration and invasion. Since IL22RA1 was expressed by MSCs and its expression was significantly increased following co-culture with C6 glioma cells, the biological functions of IL22 were investigated. Therefore, proliferation assays were performed with exogenous IL22 in FBS-free or 10% FBS DMEM/F12 medium. A 24 and 48 h incubation of MSCs with exogenous IL22 induced cell proliferation, as assessed with a CCK-8 assay (Fig. 5A). Previous studies revealed activation of the anti-apoptotic protein Bcl-xL by IL22 in glioblastoma (26), hepatocarcinoma (27) and lung cancer (20) cells. Therefore,

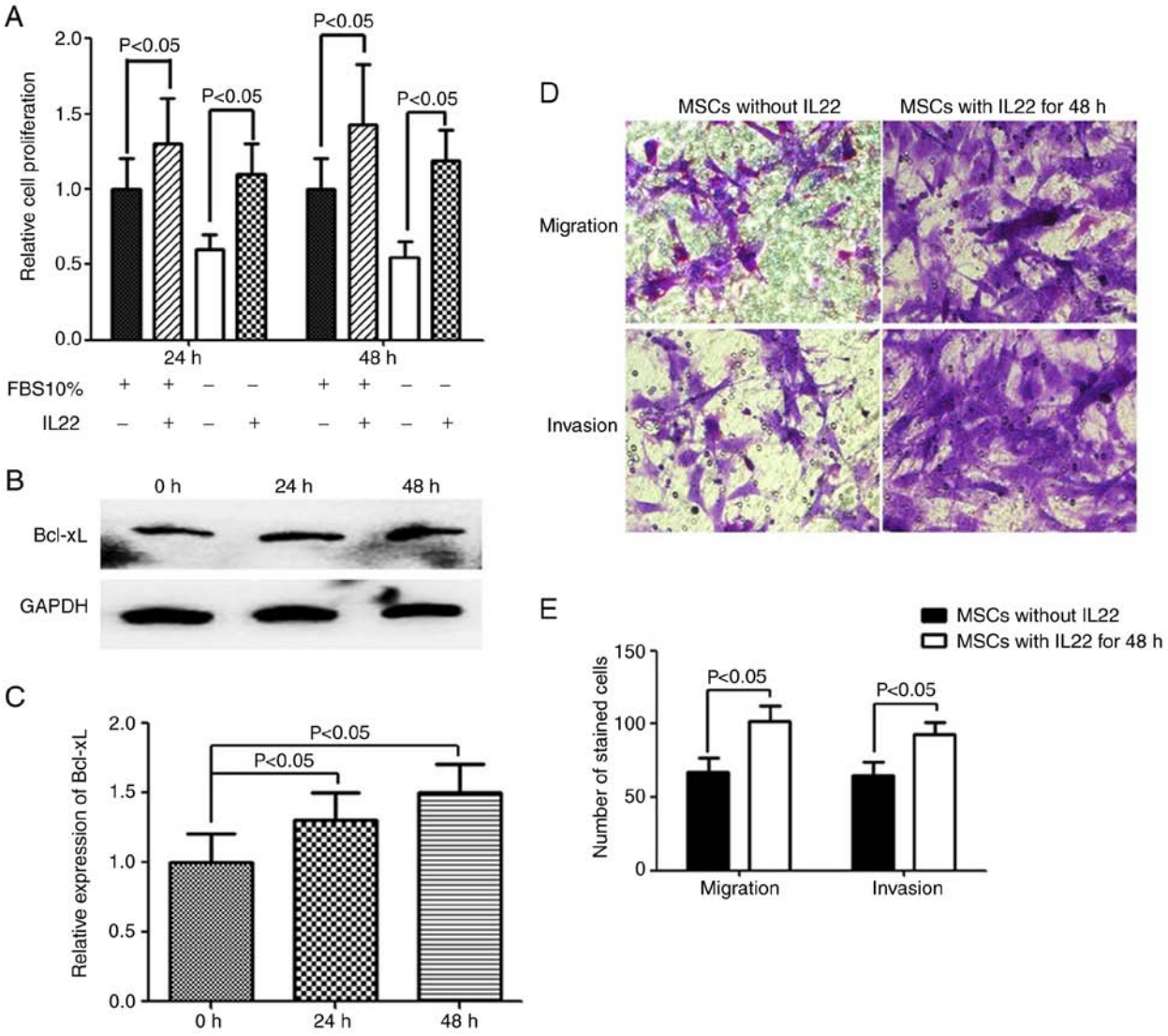

Figure 5. IL22 induce MSCs cell proliferation, migration and invasion. (A) MSCs were incubated for 24 or 48 h in basal culture DMEM/F12 medium (FBS 10%, +) and in serum-free medium (FBS 10%, -) in the presence of exogenous IL22 (+) or without IL22 (-). Cell proliferation was determined using a Cell Counting Kit-8 cell proliferation assay. (B) The anti-apoptotic factor Bcl-xL expression was assessed by western blotting (in reference to GAPDH) in total cellular protein extracted from cells treated with or without recombinant IL22 for 24 or 48 h. (C) Histogram of Bcl-xL protein expression in three groups. (D) MSCs incubated with IL22 for 48 h exhibited increased migration and invasion capacity, compared with MSCs alone. (E) Histogram of migration and invasion in two groups. FBS, fetal bovine serum; ILL22, interleukin 22; MSCs, mesenchymal stem cells; Bcl-xL, B-cell lymphoma-extra large.

the association between Bcl-xL protein and IL22 in MSCs was examined. The results revealed that IL22 increased the expression of Bcl-xL (Fig. 5B and C), which is consistent with previous studies. Furthermore, MSCs incubated with IL22 exhibited significantly increased migration and invasion capacity, compared with normal MSCs (P<0.05; Fig. 5D and E).

IL22 triggers phosphorylation of STAT3 in MSCs. To determine the signal transduction pathway induced by IL22R activation, western blot analysis was performed to measure the normal and phosphorylated forms of STAT3 (Tyr-705) in MSCs following IL22 simulation. The results demonstrated that IL22 activated STAT3 phosphorylation in MSCs, with the peak detected at 30 min (4.3-fold increase) (Fig. 6A and B). To further confirm the IL22 induction of STAT3 phosphorylation, the normal and phosphorylated forms of STAT3 were examined with immunofluorescence staining (Fig. 6C and D). The results indicated p-STAT3 nuclear localization in MSCs after 30 min of treatment, demonstrating that IL22 induced STAT3 activation and nuclear translocation.

Effect of inhibition of STAT3. To investigate the role of STAT3 pathway activation in MSCs under IL22 treatment, MSCs treated with IL22 were transfected with si-STAT3 or non-targeting control siRNA. Analyses using western blotting (Fig. 7A and B) and immunofluorescence (Fig. 7C and D) indicated that the expression levels of STAT3, p-STAT3, cyclin D1 and Bcl-xL were significantly decreased in the si-STAT3 treatment group, compared with the control siRNA treatment group or the without siRNA treatment group (P<0.05). Furthermore, inhibition of STAT3 signaling by si-STAT3 significantly decreased the IL22 simulation-induced increase in MSC proliferation, demonstrating that IL22 promoted the proliferation ability of MSCs via STAT3 signaling (Fig. 7E).

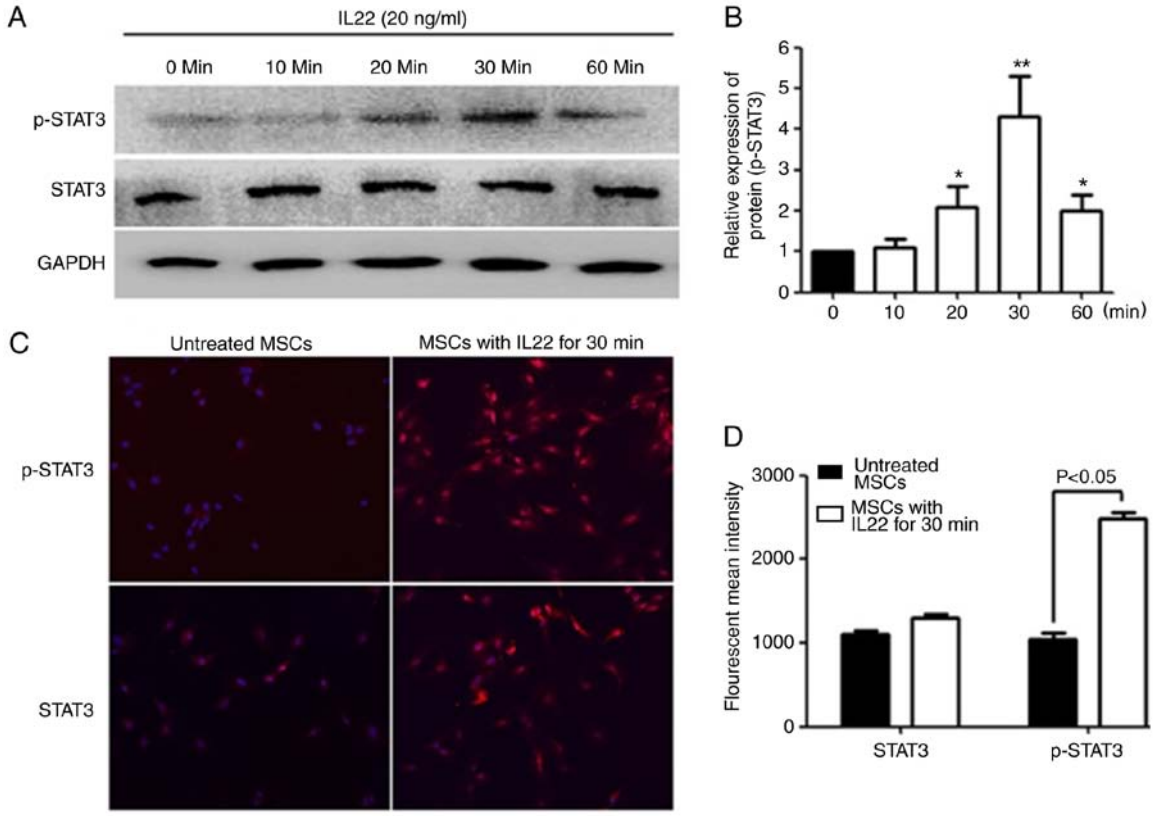

Figure 6. IL22 triggers phosphorylation of STAT3 in MSCs. (A) Following treatment with 20 ng/ml recombinant IL22 for 10, 20, 30 and 60 min, total cell lysates were assayed for STAT3 and p-STAT3 using western blot analysis. The density of each p-STAT3 band was corrected for variance in loading, using the density of the corresponding total STAT3. The expression level was evaluated as the ratio of p-STAT3 protein densities between control (0 min) and treated cells. (B) Histogram of p-STAT3 protein expression in indicated times. (C) Immunofluorescence analysis of STAT3 and p-STAT3 in MSCs between untreated or treated with IL22 for 30 min groups. Figures depict representative images for 3 repeated experiments. (D) Histogram of STAT3 and p-STAT3 protein expression in untreated or treated with IL22 for 30 min groups. *P<0.05 and **P<0.01, compared with untreated MSCs. MSCs, mesenchymal stem cells; p-STAT3, phospho-signal transducer and activator of transcription 3; IL22, interleukin 22.

Additionally, si-STAT3 significantly inhibited the migration and invasion ability of MSCs under IL22 stimulation, indicating that IL22 also promotes MSC migration and invasion through STAT3 signaling (Fig. 7F and G).

Discussion

Bone marrow-derived mesenchymal stem cells (MSCs) exhibit potent tumoritropic migratory properties that render them attractive for use as targeted-delivery vehicles in tumor treatment (6,28-35). Numerous experimental studies have confirmed the antitumor potential of MSCs modified with therapeutic genes and/or loaded with chemotherapeutic drugs (21-23). Thus, modified MSCs are a promising approach to deliver therapeutic agents to tumor niches. However, a number of contradictory reports and arguments indicated that MSCs can exert various adverse effects when they enter the tumor microenvironment (7-9,24). Chen *et al* (7) determined that MSCs can promote tumor progression on bladder cancer model. Xu *et al* (8) demonstrated that mesenchymal-stem-cell-secreted interleukin (IL)-6 enhances resistance to cisplatin via the STAT3 pathway in breast cancer. Furthermore, mesenchymal stem cell-derived IL-8 could promote osteosarcoma cell anoikis resistance and pulmonary metastasis (9). Thus, further research is required to improve the safety of this approach. Previously, it was demonstrated that MSCs directly or indirectly co-cultured with C6 glioma cells have a risk of malignant transformation and that this process may be mediated by S100B and IL6 secreted by C6 glioma cells through activation of the STAT3 pathway (7-9). However, the mechanism underlying the transformation of MSCs remains poorly understood.

IL22 is an effector cytokine that serves a major role in the regulation of inflammatory responses in a variety of tissues, including colorectal carcinogenesis, lung cancer and gastric cancer (36-39). The majority of cancer types, including gliomas, are associated with inflammation (25). Furthermore, a functional role of IL22 in carcinogenesis has been reported in colorectal, stomach and lung carcinoma, glioblastoma and hepatocarcinoma (25-29). In the present study, a gene expression database was investigated with clearly defined parameters distinguishing cancer and normal tissues. Analysis using the TCGA-GBM database revealed increased IL22RA1 mRNA expression in glioblastoma, compared with corresponding normal tissue. Investigation of the expression of IL22 and IL22RA1 in MSCs and C6 glioma cells failed to determine IL22 in the culture supernatant of C6 glioma cells or MSCs. However, the expression of IL22RA1 mRNA and protein was significantly increased in MSCs co-cultured with C6 glioma cells, compared with MSCs alone, indicating that the malignant transformation of MSCs is associated with the

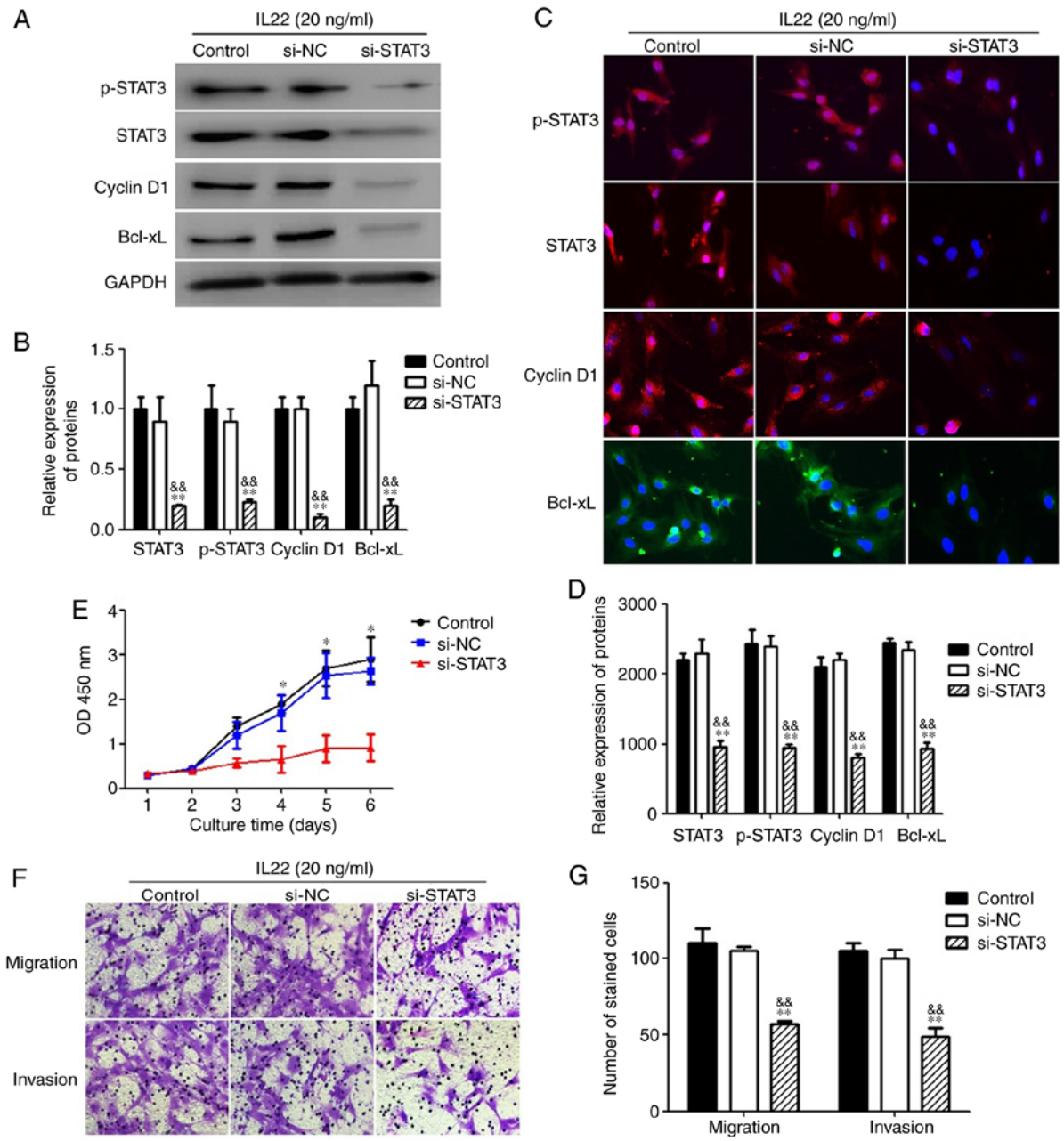

Figure 7. The suppression of upregulation of proliferation, migration and invasion by IL22 via STAT3 in MSCs. (A) MSCs treated with IL22 (20 ng/ml) were transfected with si-STAT3 (20 nM/well), non-specific siRNA (si-NC) or vehicle alone for 48 h. After transfection, total cell lysates were assayed for STAT3, p-STAT3, Cyclin D1 and Bcl-xL western blot analysis. (B) Histogram of STAT3, p-STAT3, Cyclin D1 and Bcl-xL protein expression in three groups. (C) The immunofluorescence staining depicts the significant downregulation of STAT3, p-STAT3, Cyclin D1 and Bcl-xL in MSCs treated with IL22 after transfection with si-STAT3. (D) The proliferation ability was measured with a Cell Counting Kit-8 assay. (E) The migration and invasion abilities were measured with Transwell and Matrigel assays. (F) Histogram of migration and invasion in two groups. **P<0.01, compared with the si-NC group; $^{\&\&}$P<0.01, compared with the control group. MSCs, mesenchymal stem cells; p-STAT3, phospho-signal transducer and activator of transcription 3; IL22, interleukin 22; siRNA, small interfering RNA; Bcl-xL, B-cell lymphoma-extra large; NC, negative control; OD, optical density.

IL22/IL22RA1 signaling axis and that IL22 may be derived from immune cells in the tumor microenvironment. Thus, to clarify whether IL22 promotes the malignant transformation of MSCs, MSCs were stimulated with exogenous IL22 *in vitro*. The results demonstrated that MSCs incubated with IL22 had increased Bcl-xL expression, proliferation, migration and invasion, compared with normal MSCs.

Previous studies indicated that IL22 may activate STAT3 signaling in different types of cells (26,30,31). In this regard, it was determined that STAT3 signaling pathway is activated by IL22 in MSCs and revealed that STAT3 phosphorylation is enhanced in MSCs following IL22 simulation. Accumulating evidence indicates that IL22 can promote cell proliferation and anti-apoptosis via STAT3 signaling (26,37-43). Inhibition of STAT3 signaling by si-STAT3 suppressed the IL22-induced increase of cell proliferation, migration and invasion. Based on the aforementioned results, it was considered that the extracellular IL22/IL22RA1 interaction is responsible for the activation of STAT3 in the malignant transformation of MSCs, with activated STAT3 serving an important role in the malignant transformation of MSCs in the tumor microenvironment.

In contrast, C6 glioma cells and MSCs did not secrete IL22 but did express a functional IL22 receptor (IL22RA1). The expression of IL22 was significantly increased during the malignant transformation of MSCs, indicating that IL2 could be provided by microenvironmental cells. In addition to tumor cells, immune cells, extracellular matrix, blood vessels and cytokines constitute key parts of the glioblastoma tumor microenvironment, which can be advantageous for tumor proliferation (44). Furthermore, Th17 cell invasion has been reported in an experimental mouse model of malignant glioma as well as in human glioma (45). Therefore, it may be considered that immunocompetent cells can interact with MSCs and secrete IL22 to promote the malignant transformation of MSCs. Combined with our previous findings (17,26,27), the present study indicates that IL6 secreted by C6 glioma cells may share signaling pathways with IL22, which serve a synergistic role in promoting the malignant transformation of MSCs.

In the present study, the aim was to investigate the effect and mechanism of IL22 upregulation in cell-based experiments *in vitro* as a preliminary investigation. However, animal studies on IL22RA1 upregulation and knockout or inhibition could better reveal the association between IL22/IL22RA1 and the malignant transformation of MSCs, and thus should be performed in future studies.

Acknowledgements

The authors would like to thank Professor Yi Luo of the Department of Urology, University of Iowa (Iowa, USA) for his technical support.

Funding

The present study was partially supported by a grant from the National Natural Science Foundation of China (grant no. 81670270) to JZ and the Scientific Research Project of Shanxi Provincial Department of health (grant no. 201601070) to XC.

Availability of data and materials

All data generated or analyzed during this study are included in the published article.

Authors' contributions

XC and JZ conducted the data gathering, data analyses and figure/table preparations. XJ, QY, ZX, BT, JT and JZ provided material input, data analysis and assisted with revising the manuscript. JZ supervised the experimental design and manuscript writing. All authors read and approved the final manuscript and agree to be accountable for all aspects of the research in ensuring that questions related to the accuracy or integrity of any part of the work are appropriately investigated and resolved.

Ethics approval and consent to participate

All experiments using rats were approved by the Medical Research Ethics Committee of Chongqing Medical University for the Ethics of Animal Experiments of Chongqing Medical University.

Patient consent for publication

Not applicable.

Competing interests

The authors declare that they have no competing interests.

References

1. Noh H, Zhao Q, Yan J, Kong LY, Gabrusiewicz K, Hong S, Xia X, Heimberger AB and Li S: Cell surface vimentin-targeted monoclonal antibody 86C increases sensitivity to temozolomide in glioma stem cells. Cancer Lett 433: 176-185, 2018.
2. Yan L, Cai K, Sun K, Gui J and Liang J: MiR-1290 promotes proliferation, migration, and invasion of glioma cells by targeting *LHX6*. J Cell Physiol 233: 6621-6629, 2018.
3. Wang K, Huang R, Li G, Zeng F, Zhao Z, Liu Y, Hu H and Jiang T: CKAP2 expression is associated with glioma tumor growth and acts as a prognostic factor in highgrade glioma. Oncol Rep 40: 2036-2046, 2018.
4. Sun Z, Wang S and Zhao RC: The roles of mesenchymal stem cells in tumor inflammatory microenvironment. J Hematol Oncol 7: 14, 2014.
5. Razmkhah M, Abtahi S and Ghaderi A: Mesenchymal stem cells, immune cells and tumor cells cross talk: A sinister triangle in the tumor microenvironment. Curr Stem Cell Res Ther 14: 43-51, 2019.
6. Xu S, De Veirman K, De Becker A, Vanderkerken K and Van Riet I: Mesenchymal stem cells in multiple myeloma: A therapeutical tool or target? Leukemia 32: 1500-1514, 2018.
7. Chen J, Ma L, Zhang N, Zhu Y, Zhang K, Xu Z and Wang Q: Mesenchymal stem cells promote tumor progression via inducing stroma remodeling on rabbit VX2 bladder tumor model. Int J Biol Sci 14: 1012-1021, 2018.
8. Xu H, Zhou Y, Li W, Zhang B, Zhang H, Zhao S, Zheng P, Wu H and Yang J: Tumor-derived mesenchymal-stem-cell-secreted IL-6 enhances resistance to cisplatin via the STAT3 pathway in breast cancer. Oncol Lett 15: 9142-9150, 2018.
9. Du L, Han XG, Tu B, Wang MQ, Qiao H, Zhang SH, Fan QM and Tang TT: CXCR1/Akt signaling activation induced by mesenchymal stem cell-derived IL-8 promotes osteosarcoma cell anoikis resistance and pulmonary metastasis. Cell Death Dis 9: 714, 2018.
10. Rosland GV, Svendsen A, Torsvik A, Sobala E, McCormack E, Immervoll H, Mysliwietz J, Tonn JC, Goldbrunner R, Lønning PE, *et al*: Long-term cultures of bone marrow-derived human mesenchymal stem cells frequently undergo spontaneous malignant transformation. Cancer Res 69: 5331-5339, 2009.
11. Tan B, Shen L, Yang K, Huang D, Li X, Li Y, Zhao L, Chen J, Yi Q, Xu H, *et al*: C6 glioma-conditioned medium induces malignant transformation of mesenchymal stem cells: Possible role of S100B/RAGE pathway. Biochem Biophys Res Commun 495: 78-85, 2018.
12. Cui X, Liu J, Bai L, Tian J and Zhu J: Interleukin-6 induces malignant transformation of rat mesenchymal stem cells in association with enhanced signaling of signal transducer and activator of transcription 3. Cancer Sci 105: 64-71, 2014.
13. Liu J, Zhang Y, Bai L, Cui X and Zhu J: Rat bone marrow mesenchymal stem cells undergo malignant transformation via indirect co-cultured with tumour cells. Cell Biochem Funct 30: 650-656, 2012.
14. Morisse MC, Jouannet S, Dominguez-Villar M, Sanson M and Idbaih A: Interactions between tumor-associated macrophages and tumor cells in glioblastoma: Unraveling promising targeted therapies. Expert Rev Neurother 18: 729-737, 2018.
15. Broekman ML, Maas SL, Abels ER, Mempel TR, Krichevsky AM and Breakefield XO: Multidimensional communication in the microenvirons of glioblastoma. Nat Rev Neurol 14: 482-495, 2018.

16. Mukherjee S, Fried A, Hussaini R, White R, Baidoo J, Yalamanchi S and Banerjee P: Phytosomal curcumin causes natural killer cell-dependent repolarization of glioblastoma (GBM) tumor-associated microglia/macrophages and elimination of GBM and GBM stem cells. J Exp Clin Cancer Res 37: 168, 2018.
17. He W, Wu J, Shi J, Huo YM, Dai W, Geng J, Lu P, Yang MW, Fang Y, Wang W, *et al*: IL22RA1/STAT3 signaling promotes stemness and tumorigenicity in pancreatic cancer. Cancer Res 78: 3293-3305, 2018.
18. Xie XJ, Di TT, Wang Y, Wang MX, Meng YJ, Lin Y, Xu XL, Li P and Zhao JX: Indirubin ameliorates imiquimod-induced psoriasis-like skin lesions in mice by inhibiting inflammatory responses mediated by IL-17A-producing gd T cells. Mol Immunol 101: 386-395, 2018.
19. Livak KJ and Schmittgen TD: Analysis of relative gene expression data using real-time quantitative PCR and the $2^{-\Delta\Delta C_T}$ method. Methods 25: 402-408, 2001.
20. Endam LM, Bossé Y, Filali-Mouhim A, Cormier C, Boisvert P, Boulet LP, Hudson TJ and Desrosiers M: Polymorphisms in the interleukin-22 receptor alpha-1 gene are associated with severe chronic rhinosinusitis. Otolaryngol Head Neck Surg 140: 741-747, 2009
21. Shall G, Menosky M, Decker S, Nethala P, Welchko R, Leveque X, Lu M, Sandstrom M, Hochgeschwender U, Rossignol J, *et al*: Effects of passage number and differentiation protocol on the generation of dopaminergic neurons from rat bone marrow-derived mesenchymal stem cells. Int J Mol Sci 19: pii: E720, 2018.
22. Li H and Chen C: Quercetin Has Antimetastatic Effects on Gastric Cancer Cells via the Interruption of uPA/uPAR Function by Modulating NF-κb, PKC-δ, ERK1/2, and AMPKα. Integr Cancer Ther 17: 511-523, 2018.
23. Chen D, Zou J, Zong Y, Meng H, An G and Yang L: Anti-human CD138 monoclonal antibodies and their bispecific formats: Generation and characterization. Immunopharmacol Immunotoxicol 38: 175-183, 2016.
24. Liakou E, Mavrogonatou E, Pratsinis H, Rizou S, Evangelou K, Panagiotou PN, Karamanos NK, Gorgoulis VG and Kletsas D: Ionizing radiation-mediated premature senescence and paracrine interactions with cancer cells enhance the expression of syndecan 1 in human breast stromal fibroblasts: The role of TGF-β. Aging 8: 1650-1669, 2016.
25. Boniface K, Guignouard E, Pedretti N, Garcia M, Delwail A, Bernard FX, Nau F, Guillet G, Dagregorio G, Yssel H, *et al*: A role for T cell-derived interleukin 22 in psoriatic skin inflammation. Clin Exp Immunol 150: 407-415, 2007.
26. Akil H, Abbaci A, Lalloué F, Bessette B, Costes LM, Domballe L, Charreau S, Guilloteau K, Karayan-Tapon L, Bernard FX, *et al*: IL22/IL-22R pathway induces cell survival in human glioblastoma cells. PLoS One 10: e0119872, 2015.
27. Jiang R, Tan Z, Deng L, Chen Y, Xia Y, Gao Y, Wang X and Sun B: Interleukin-22 promotes human hepatocellular carcinoma by activation of STAT3. Hepatology 54: 900-909, 2011.
28. Zhang W, Chen Y, Wei H, Zheng C, Sun R, Zhang J and Tian Z: Antiapoptotic activity of autocrine interleukin-22 and therapeutic effects of interleukin-22-small interfering RNA on human lung cancer xenografts. Clin Cancer Res 14: 6432-6439, 2008.
29. Corsten MF and Shah K: Therapeutic stem-cells for cancer treatment: Hopes and hurdles in tactical warfare. Lancet Oncol 9: 376-384, 2008.
30. Qian J, Hu Y, Zhao L, Xia J, Li C, Shi L and Xu F: Protective role of adipose-derived stem cells in *Staphylococcus aureus*-induced lung injury is mediated by RegIIIγ secretion. Stem Cells 34: 1947-1956, 2016.
31. Xu F, Hu Y, Zhou J and Wang X: Mesenchymal stem cells in acute lung injury: Are they ready for translational medicine? J Cell Mol Med 17: 927-935, 2013.
32. Ahn Jo, Lee Hw, Seo Kw, Kang Sk, Ra Jc and Youn Hy: Anti-tumor effect of adipose tissue derived-mesenchymal stem cells expressing interferon-β and treatment with cisplatin in a xenograft mouse model for canine melanoma. PLoS One 8: e74897, 2013.
33. Xu G, Guo Y, Seng Z, Cui G and Qu J: Bone marrow-derived mesenchymal stem cells co-expressing interleukin-18 and interferon-β exhibit potent antitumor effect against intracranial glioma in rats. Oncol Rep 34: 1915-1922, 2015.
34. Studeny M, Marini FC, Champlin RE, Zompetta C, Fidler IJ and Andreeff M: Bone marrow-derived mesenchymal stem cells as vehicles for interferon-beta delivery into tumors. Cancer Res 62: 3603-3608, 2002.
35. He X, Li B, Shao Y, Zhao N, Hsu Y, Zhang Z and Zhu L: Cell fusion between gastric epithelial cells and mesenchymal stem cells results in epithelial-to-mesenchymal transition and malignant transformation. BMC Cancer 15: 24, 2015.
36. Leyva-Castillo JM, Yoon J and Geha RS: IL-22 promotes allergic airway inflammation in epicutaneously sensitized mice. J Allergy Clin Immunol: Jun 18, 2018 (Epub ahead of print). pii: S0091-6749(18)30856-X. doi: 10.1016/j.jaci.2018.05.032.
37. Khare V, Paul G, Movadat O, Frick A, Jambrich M, Krnjic A, Marian B, Wrba F and Gasche C: IL10R2 overexpression promotes IL22/STAT3 signaling in colorectal carcinogenesis. Cancer Immunol Res 3: 1227-1235, 2015.
38. Shen Z, Ye Y, Kauttu T, Seppänen H, Vainionpää S, Wang S, Mustonen H and Puolakkainen P: The novel focal adhesion gene kindlin-2 promotes the invasion of gastric cancer cells mediated by tumor-associated macrophages. Oncol Rep 29: 791-797, 2013.
39. Khosravi N, Caetano MS, Cumpian AM, Unver N, De la Garza Ramos C, Noble O, Daliri S, Hernandez BJ, Gutierrez BA, Evans SE, *et al*: IL22 promotes Kras-Mutant lung cancer by induction of a protumor immune response and protection of stemness properties. Cancer Immunol Res 6: 788-797, 2018.
40. Chen E, Cen Y, Lu D, Luo W and Jiang H: IL-22 inactivates hepatic stellate cells via downregulation of the TGF-β1/Notch signaling pathway. Mol Med Rep 17: 5449-5453, 2018.
41. Yeste A, Mascanfroni ID, Nadeau M, Burns EJ, Tukpah AM, Santiago A, Wu C, Patel B, Kumar D and Quintana FJ: IL-21 induces IL-22 production in CD4+ T cells. Nat Commun 5: 3753, 2014.
42. Guo X, Qiu J, Tu T, Yang X, Deng L, Anders RA, Zhou L and Fu YX: Induction of innate lymphoid cell-derived interleukin-22 by the transcription factor STAT3 mediates protection against intestinal infection. Immunity 40: 25-39, 2014.
43. Zhang B, Xie S, Su Z, Song S, Xu H, Chen G, Cao W, Yin S, Gao Q and Wang H: Heme oxygenase-1 induction attenuates imiquimod-induced psoriasiform inflammation by negative regulation of Stat3 signaling. Sci Rep 6: 21132, 2016.
44. Zhu VF, Yang J, Lebrun DG and Li M: Understanding the role of cytokines in Glioblastoma Multiforme pathogenesis. Cancer Lett 316: 139-150, 2012.
45. Wainwright DA, Sengupta S, Han Y, Ulasov IV and Lesniak MS: The presence of IL-17A and T helper 17 cells in experimental mouse brain tumors and human glioma. PLoS One 5: e15390, 2010.

This work is licensed under a Creative Commons Attribution-NonCommercial-NoDerivatives 4.0 International (CC BY-NC-ND 4.0) License.